Conversion of Colloidal Crystals to Polymer Nets: Turning Latex Particles Inside Out

Yiyan Chen,† Warren T. Ford,*,† Nicholas F. Materer,† and Dale Teeters‡

Department of Chemistry, Oklahoma State University, Stillwater, Oklahoma 74078, and Department of Chemistry and Biochemistry, University of Tulsa, Tulsa, Oklahoma 74104

Received March 19, 2001. Revised Manuscript Received June 4, 2001

Copolymer latexes of styrene and 5−10 mol % 2-hydroxyethyl methacrylate (HEMA) with narrow polydispersity produce films of colloidal crystals on glass by evaporative deposition. Treatment with vapors of styrene or toluene followed by drying transforms the morphology of the film to a porous polymer net with hexagonally ordered holes on the surface. We propose that the conversion takes place by swelling of styrene into the polystyrene-rich cores of the particles, which expand and engulf the polyHEMA-rich shells, leaving the polystyrene-rich phase on the surface and the polyHEMA-rich phase inside after the styrene evaporates. Evidence for the polyHEMA-rich surface of the colloidal crystal and the polystyrene-rich surface of the net is provided by contact angle measurements that show the surface of the net to be more hydrophobic than the colloidal crystal and by X-ray photoelectron spectroscopic measurements that show a higher oxygen content on the surface of the colloidal crystal than on the surface of the net.

Introduction

Materials with three-dimensional order on a submicrometer scale have many potential applications as, for example, photonic band gap materials,[1] size-selective membranes,[2] and microchip reactors.[3] Colloidal crystals of monodisperse silica or polymer latex particles are one way of achieving such ordered materials.[4,5] A colloidal crystal is analogous to a molecular crystal, but the building blocks are colloidal particles instead of molecules. There are two categories of self-assembly of colloidal particles. Charged particles in a fluid such as water repel one another over long distances, forming bcc unit cells at low particle concentrations and fcc unit cells or randomly stacked hexagonal planes at higher particle concentrations. Only charged particles larger than 70 nm in diameter are known to form colloidal crystals at low concentrations. Brownian motion prevents smaller particles from settling into a fixed lattice space. Colloidal spheres can also pack tightly into fcc crystals in which the spheres occupy 74% of the volume. Low polydispersity of the particles is critical for colloidal crystal formation at both low and high particle concentrations. Uniform size also means uniform charge because all particles in a sample have the same surface charge density.

Colloidal crystals are iridescent as a result of Bragg diffraction of visible light. They have been known for two millenia in the form of opals, which are composed of silica spheres of higher density in a matrix of lower-density silica.[6] Currently, both natural and synthetic opals are used in jewelery. Because of Bragg diffraction, colloidal crystals can be narrow-bandwidth optical filters.[7,8] When the lattice dimension is changed by temperture, radiation, or mechanical stress, they can be optical switches,[9,10] and when the lattice dimension is changed by a chemical stimulus, they can be chemical sensors.[11,12] Solid colloidal crystals can be obtained via densely packed spheres or polymerization of the liquid medium around the particles in dilute colloidal crystalline arrays.[8,10,13] Close-packed colloidal crystals have been made by filtration[14] and by evaporation of the fluid to deposit a film on either horizontal[15] or nearly vertical solid substrates.[16] The rate of deposition can be increased by flow,[17] by an electric field,[18,19] or by oscilla-

* To whom correspondence should be addressed. E-mail: wtford@okstate.edu.
† Oklahoma State University.
‡ University of Tulsa.

(1) Joannopoulos, J. D.; Meade, R. D.; Winn, J. N. *Photonic Crystals: Molding the Flow of Light*; Princeton University Press: Princeton, NJ, 1995.
(2) Baker, R. W.; Cussler, E. L.; Eykamp, W.; Koros, W. J.; Riley, R. L.; Strathmann, H. *Membrane Separation Systems: Recent Developments and Future Directions*; Noyes Data Corporation: Park Ridge, NJ, 1991.
(3) Gau, H.; Herminghaus, S.; Lenz, P.; Lipowsky, R. *Science* **1999**, *283*, 46.
(4) Grier, D. G., Ed. *From Dynamics to Devices: Directed Self-Assembly of Colloidal Materials*, *MRS Bulletin*; Materials Research Society: Warrendale, PA, 1998; Vol. 23, No. 10.
(5) Gast, A. P.; Russel, W. B. *Phys. Today* **1998**, *51*, 24.
(6) Nassau, K. *Gems Made by Man*; Chilton Book Company: Radnor, PA, 1980.
(7) Carlson, R. J.; Asher, S. A. *Appl. Spectrosc.* **1984**, *38*, 297.
(8) Sunkara, H. B.; Jethmalani, J. M.; Ford, W. T. *Chem. Mater.* **1994**, *6*, 362.
(9) Kesavamoorthy, R.; Super, M. S.; Asher, S. A. *J. Appl. Phys.* **1992**, *71*, 1116.
(10) Weissman, J. M.; Sunkara, H. B.; Tse, A. S.; Asher, S. A. *Science* **1996**, *274*, 959.
(11) Holtz, J. H.; Asher, S. A. *Nature* **1997**, *389*, 829.
(12) Lee, K.; Asher, S. A. *J. Am. Chem. Soc.* **2000**, *122*, 9534.
(13) Jethmalani, J. M.; Ford, W. T. *Chem. Mater.* **1996**, *8*, 2138.
(14) Holland, B. T.; Blanford, C.; Stein, A. *Science* **1998**, *281*, 538.
(15) Dushkin, C. D.; Lazarov, G. S.; Kotsev, S. N.; Yoshimura, H.; Nagayama, K. *Colloid Polym. Sci.* **1999**, *277*, 914.
(16) Jiang, P.; Bertone, J. F.; Hwang, K. S.; Colvin, V. L. *Chem. Mater.* **1999**, *11*, 2132.
(17) Park, S. H.; Xia, Y. *Langmuir* **1999**, *15*, 266.

10.1021/cm010255r CCC: $20.00
Published on Web 07/06/2001

tory shear.[20] Epitaxial crystallization can be promoted by use of a substrate having holes[21] or grooves[17,22] matched to the desired crystal lattice.

Solid colloidal crystals of silica and of polymer spheres have been transformed into other periodic structures. The interstitial spaces have been filled with materials such as sol−gel precursors to metal oxides, polymerizable monomers, and nanometer-sized colloidal metals, metal oxides, or semiconductors. Solidification of the filler followed by removal of the silica or polymer spheres using either chemical erosion or calcination has produced inverse opals, consisting of regular holes in solid lattices of metal oxides, metals, semiconductors, and various polymers.[23,24] If there is a large enough contrast of the refractive indices of the lattice and the voids, and if the voids are perfectly ordered, then the inverse opal should exhibit a complete photonic band gap.[1,23−26] With much less than perfect order, the holey materials could be highly selective membranes.

We have discovered a new way to convert colloidal crystalline films of polymer latexes into porous polymer nets having ordered holes spaced at the same distance as in the colloidal crystal. Preliminary results on the conversion and Bragg diffraction of both the colloidal crystal and the net have been reported.[27] In this paper, we archive the experimental procedure for the conversion, propose a model to explain the morphological transformation, and report details of surface wetting and XPS (X-ray photoelectron spectroscopy) experiments and of seed-growth and starved-growth emulsion polymerization experiments to support the model. The nets have potential as photonic band gap materials, templates for epitaxial crystallization, membranes, and catalyst supports. The process consists of swelling the polymer by exposure to solvent vapors to increase its mobility, spontaneous reorganization of the polymer toward a new swollen equilibrium state, and deswelling into the new morphology. It is related to the formation of periodic equilibrium structures of block copolymers, which usually have a smaller length scale that is determined by the lengths of the blocks. The dimensions of colloidal crystals are generally hundreds of nanometers, whereas those of block copolymers are tens of nanometers.[28,29] However, some block copolymers organize at longer length scales. One type of rod−coil block copolymers forms periodic arrays of micrometer-sized holes in solid matrixes.[30] Block copolymers blended with one homopolymer are also promising as precursors to photonic band gap materials with lattice dimensions of hundreds of nanometers.[31]

Experimental Section

Materials. Styrene and 2-hydroxyethyl methacrylate (HEMA) from Aldrich Chemical Co. were distilled under reduced pressure and stored at −40 °C. Potassium persulfate (KPS) and 2,2′-azobisisobutyronitrile (AIBN) were used as received from Aldrich. Water was deionized and treated with active carbon in a Barnsted ultrapure system to a resistivity of $>10^6$ Ω cm after exposure to air. All glassware, microscope slides, and cover slips were soaked in a KOH/ethanol bath for at least overnight, rinsed thoroughly with deionized water, and dried in an oven. The slides and cover slips were covered to protect them from dust.

Measurements. Transmission electron microscopy (TEM) images were obtained with a JEOL JEM 100 C × II instrument (Tokyo, Japan) at 80 keV. Scanning electron microscopy (SEM) experiments were performed with JEOL JXM 6400 (Tokyo, Japan) equipment. Both TEM and SEM samples were observed without staining. SEM samples were coated with gold/palladium to improve conductivity. Cross-section samples of colloidal crystal films on glass were obtained at room temperature by fracture of the film on glass with the glass scored on one side. Most cross-section samples of solvent-treated nets were fractured in liquid nitrogen to minimize tear deformation. X-ray photoelectron spectroscopy (XPS) employed a double-pass cylindrical mirror analyzer with a pass energy of 100 eV, a Mg Kα source, and an angle of 45° between the sample and the analyzer. Vacuum was maintained by an ion pump at a pumping rate of 330 L s^{-1}. The wetting behavior of the colloidal crystalline and net films was measured by the dynamic Wilhelmy plate method.[32] Barnstead ultrapure water was used for all wetting studies.

Poly(HEMA-*co*-styrene). Latexes containing 1−10 mol % HEMA were prepared by batch emulsion polymerizations following the literature procedure.[33] The dispersions were filtered with a 70−100-μm fritted funnel and then dialyzed with a daily change of the water for 2 months. Colloidal sphere diameters were measured from at least two TEM images of each sample and averaged over 40 spheres.

Starved Addition Polymerization. An emulsion polymerization with 90 mol % styrene (1.04 g, 10.0 mmol) and 10% HEMA (0.150 g, 1.15 mmol) and 0.1 mol % KPS (0.0362 g, 0.130 mmol) initiator in 20.0 mL of water was started at 70 °C. After 3 h, 2.08 g (20.0 mmol) of styrene was added using a syringe pump at a rate of 1.00 mL h^{-1}. The reaction was continued for a total time of 10 h.

Seed-Growth Polymerization. At 25 °C, 1.04 g (10.0 mmol) of styrene was added at a rate of 1.00 mL h^{-1} with a syringe pump to 20.0 mL of a stirred 5 wt % solids/10 mol % HEMA latex. After the mixture was stirred overnight, 0.100 mmol of KPS or AIBN was added. The mixture was stirred for 40 min and then heated to 70 °C for 8 h.

Colloidal Crystals.[16] A glass slide was placed vertically in a vial of latex of approximately 0.5 wt % concentration. The vial was placed in a covered Erlenmeyer flask with a glass T tube at the mouth. Untreated house compressed air was passed through the T tube to accelerate the evaporation. Over 2 days, a 25-mm iridescent band of colloidal crystals deposited on the glass slide as well as on the inner wall of the vial. The thickness of the colloidal film depended on the concentration of latex in the dispersion. A 0.5% dispersion usually gave a well-ordered film with a thickness of about 13−17 layers. With higher concentrations, the films were less ordered. With 0.1%

(18) Holgado, M.; Garcia-Santamaria, F.; Blanco, A.; Ibisate, M.; Cintas, A.; Miguez, H.; Serna, C. J.; Molpeceres, C.; Requena, J.; Mifsud, A.; Meseguer, F.; Lopez, C. *Langmuir* **1999**, *15*, 4701.
(19) Rogach, A. L.; Kotov, N. A.; Koktysh, D. S.; Ostrander, J. W.; Ragoisha, G. A. *Chem. Mater.* **2000**, *12*, 2721.
(20) Vickreva, O.; Kalinina, O.; Kumacheva, E. *Adv. Mater.* **2000**, *12*, 110.
(21) van Blaaderen, A.; Rue, R.; Wiltzius, P. *Nature* **1997**, *385*, 321.
(22) Mayers, B. T.; Gates, B.; Xia, Y. *Adv. Mater.* **2000**, *12*, 1629.
(23) Xia, Y.; Gates, B.; Yin, Y.; Lu, Y. *Adv. Mater.* **2000**, *12*, 693.
(24) Velev, O. D.; Lenhoff, A. M. *Curr. Opin. Colloid Interface Sci.* **2000**, *5*, 56.
(25) Yablonovitch, E. *Phys. Rev. Lett.* **1987**, *58*, 2059.
(26) John, S. *Phys. Rev. B: Condens. Matter* **1987**, *35*, 9291.
(27) Chen, Y.; Ford, W. T.; Materer, N. F.; Teeters, D. *J. Am. Chem. Soc.* **2000**, *122*, 10472.
(28) Noshay, A.; McGrath, J. E. *Block Copolymers: Overview and Critical Survey*; Academic Press: New York, 1977.
(29) Hamley, I. W. *The Physics of Block Copolymers*; Oxford University Press: New York, 1998.
(30) Jenekhe, S. A.; Chen, X. L. *Science* **1999**, *283*, 372.
(31) Chan, V. Z. H.; Hoffman, J.; Lee, V. Y.; Iatrou, H.; Avgeropoulos, A.; Hadjichristidis, N.; Miller, R. D.; Thomas, E. L. *Science* **1999**, *286*, 1716.
(32) Teeters, D.; Wilson, J. F.; Andersen, M. A.; Thomas, D. C. *J. Colloid Interface Sci.* **1988**, *126*, 641.
(33) Cardoso, A. H.; Leite, C. A. P.; Galembeck, F. *Langmuir* **1999**, *15*, 5, 4447.

Table 1. Compositions and Sizes of Styrene−HEMA Copolymer Latexes

% HEMA	diameter (nm)[a]
10	369 ± 13
5	424 ± 12
1	365 ± 8

[a] Measured from TEM images; value ± standard deviation.

or lower concentration, monolayer films formed in patches on the glass slide.

Preparation of a Polymer Net. Styrene or toluene was placed in the bottom of a glass jar, a glass slide coated with the colloidal crystalline film was placed in the jar 10 mm above the solvent, and the jar was sealed for 3 h or more at room temperature (22−30 °C). The white colloidal crystalline film gradually changed to a transparent polymer film. The glass slide was taken out of the chamber and dried at room temperature in the air.

Results and Discussion

Styrene−HEMA Copolymer Latexes. Emulsion polymerization of hydrophilic with hydrophobic monomers can lead to amphiphilic copolymers. Amphiphilic styrene−HEMA copolymer latexes form colloidal crystals with exceptional ease.[34] We prepared 35 latexes with different compositions and morphologies by batch emulsion copolymerizations initiated with potassium persulfate at 70 °C. Three samples are listed in Table 1. The emulsion polymerization is initiated and chain propagation begins in the aqueous phase. When the growing chain becomes insoluble, it forms a micellar particle with the hydrophobic styrene units inside and the hydrophilic HEMA repeat units mainly on the hydrated surface. Because of its solubility in water, HEMA is consumed early in the process.[35] After consumption of most of the HEMA, continued polymerization of styrene and possibly some residual HEMA enlarges the polystyrene cores of the particles. The raspberry-like texture of the spheres with high HEMA contents (Figure 1A) is probably due to phase separation and formation of polyHEMA-rich domains on the surface during drying.[33,34] With decreasing HEMA content, the latex spheres become smoother (Figure 1B and C). Polymerization of samples with HEMA contents higher than 10 mol % failed to form isolated colloid particles. Interfacial elemental concentration measurements using X-ray photoelectron spectroscopy (XPS) and energy loss of scattered electrons while scanning in a TEM support a high oxygen content on the particle surface.[33,36]

Colloidal Crystals. The latex particles formed colloidal crystalline layers on glass microscope slides or cover slips by vertical evaporative deposition[16] from a 0.5% solids dispersion over 2 days at 25 °C with a stream of air passing over the headspace of the growth chamber. The bands of colloidal crystals on glass were up to 25 mm long and were highly iridescent, appearing green, blue, purple, or pink depending on the viewing angle. The SEM images in Figure 2 show colloidal crystals with the hexagonal (111) planes parallel to the

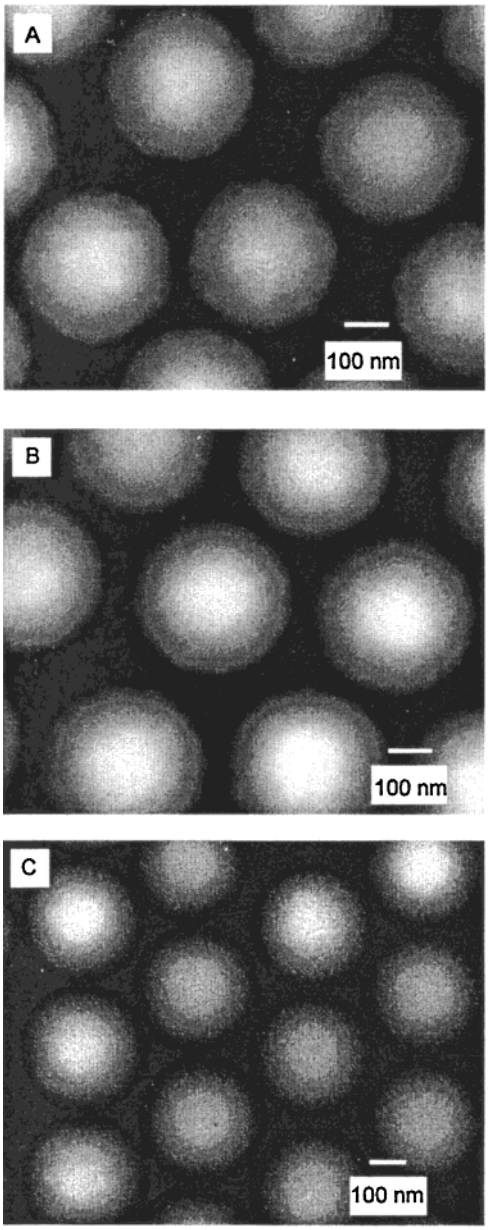

Figure 1. TEM images of poly(HEMA-*co*-styrene) latexes: (A) 90% styrene and 10% HEMA, (B) 95% styrene and 5% HEMA, (C) 99% styrene and 1% HEMA.

substrate, as reported before for polystyrene spheres deposited by evaporation onto glass.[34,37] Also as reported before, the individual particles appear as rounded hexagons rather than perfect circles; the spacings of the particles along the three axes passing through centers of adjacent particles are not equal, and lines along those axes drawn through the centers of the particles are slightly curved.[38] These observations have been attributed to swelling of the particles.[38] The colloidal crystalline films are increasingly robust with increasing HEMA content. A pristine film of the 10 mol % HEMA copolymer adheres to glass when dropped or washed.

Porous Polymer Net. Opaque colloidal crystalline films on glass slides were treated with vapor of styrene

(34) Cardoso, A. H.; Leite, C. A. P.; Zaniquelli, M. E. D.; Galembeck, F. *Colloids Surf. A* **1998**, *144*, 207.
(35) Kamei, S.; Okubo, M.; Matsumoto, T. *J. Polym. Sci., Part A: Polym. Chem.* **1986**, *24*, 3109.
(36) Okubo, M.; Yamamoto, Y.; Kamei, S. *Colloid Polym. Sci.* **1989**, *267*, 861.
(37) Rogach, A.; Susha, A.; Caruso, F.; Sukhorukov, G.; Kornowski, A.; Kershaw, S.; Mohwald, H.; Eychmuller, A.; Weller, H. *Adv. Mater.* **2000**, *12*, 333.
(38) Galembeck, A.; Costa, C. A. R.; Medeiros da Silva, M. d. C. V.; Galembeck, F. *J. Colloid Interface Sci.* **2001**, *234*, 393−399.

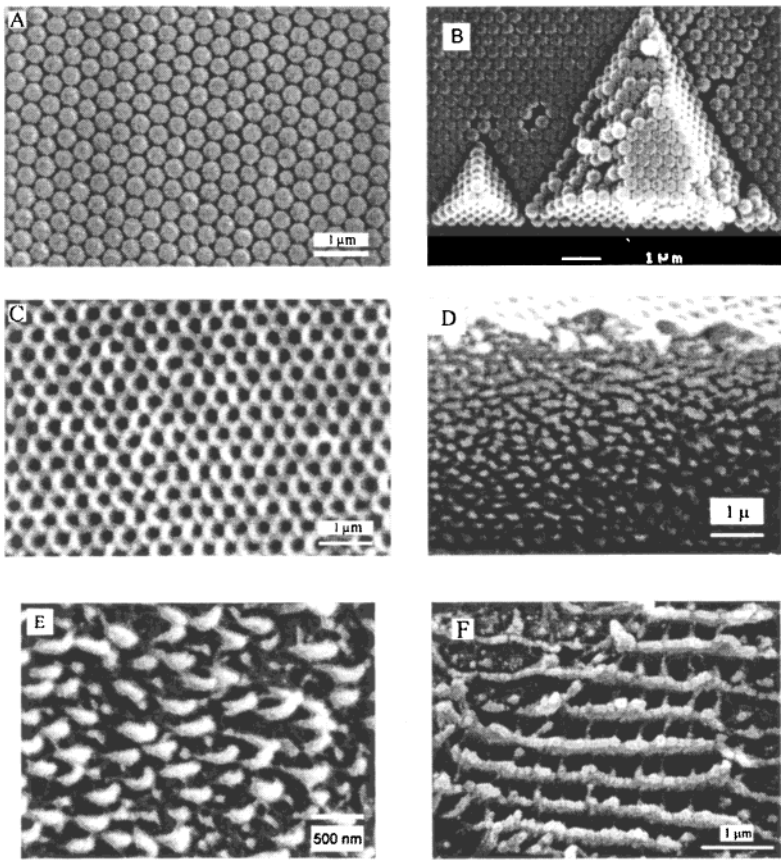

Figure 2. SEM images of colloidal crystals and polymer nets. All samples contained 10% HEMA and were made from 369-nm particles. (A) Top surface of a colloidal crystal. (B) Internal surfaces exposed by fracture of a film showing pyramids of packed spheres. Surfaces parallel to the substrate are (111) hexagonal facets. The (100) square facets form a 125.3° angle with the hexagonal planes. (C) The top surface of the net has a hexagonal arrangement of holes with a center-to-center distance of 370 nm, and the holes are about 300 nm in diameter. (D,E) Cross-sectional views of net samples fractured at slightly lower than ambient temperature. (F) Cross section of a sample fractured in liquid nitrogen showing a tetragonal pattern of holes.

or toluene. After being allowed to dry in air at room temperature, the films appeared much less iridescent than the films of colloidal crystals, and they had a completely different morphology of a polymer net, as shown in Figure 2C−F. On the top surface (Figure 2C) the holes are arranged hexagonally at the same periodicity and the same distortions from a perfect hexagonal layer as the spheres on the surface of the colloidal crystal. Several different cross-sectional views of the net are shown. For Figure 2D and E, the samples were broken at close to ambient temperature, and the polymer nets appear to be torn apart. Figure 2D shows a general view of the porosity of the cross section, whereas Figure 2E shows some loop structures, which are the building blocks of the polymer net. The sample for Figure 2F was fractured in liquid nitrogen and is less distorted by tearing. It shows holes with tetragonal order. Macroscopic observations also indicate that three-dimensional order of the colloidal crystal was partially maintained in the net. The net films are slightly iridescent and have a weak but distinct absorption peak in the visible−near-infrared transmission spectra as a result of Bragg diffraction.[27] The nets stick to glass even when the glass has been fractured, and they are much less brittle than nonporous homopolystyrene films.

The transformation of colloidal crystal to net succeeded with styrene and toluene, which are good solvents for polystyrene and poor solvents for polyHEMA, but failed with chloroform, dichloromethane, and tetrahydrofuran, which are solvents for both polystyrene and polyHEMA. Variation of the HEMA content revealed that colloidal crystalline films from 10 and 5% HEMA latexes transformed to nets, but a 1% HEMA film did not. Instead, the colloidal crystal from the 1% HEMA latex was converted to a featureless continuous film. Variation of size of the particles of 10% HEMA latexes showed that colloidal crystals of all particle sizes from 200 to 480 nm in diameter were transformed to nets.

Model for the Colloidal Crystal-to-Net Transformation. We attribute the dramatic change of morphology of the films to a structural rearrangement that originates in the core−shell structure of the latexes. As depicted in Figure 3, vapors of a good solvent for polystyrene and poor solvent for polyHEMA permeate into the cores of the particles and swell the polystyrene. This lowers the glass transition temperature of the polystyrene-rich phase from 100 °C to subambient. The swollen cores cannot be contained and crack the polyHEMA shells. One of the intermediate states, where some spheres clearly have cracks, is shown in Figure 4A. The mobile, swollen, polystyrene-rich phase migrates to the air−polymer interface and engulfs the minor polyHEMA-rich phase, approaching a new swollen equilibrium morphology with holes where the cores of the spheres had been before. This process turns the latex spheres inside out. Because the polyHEMA-rich phase does not swell in styrene and is relatively immobile, treatment of the colloidal crystal with only

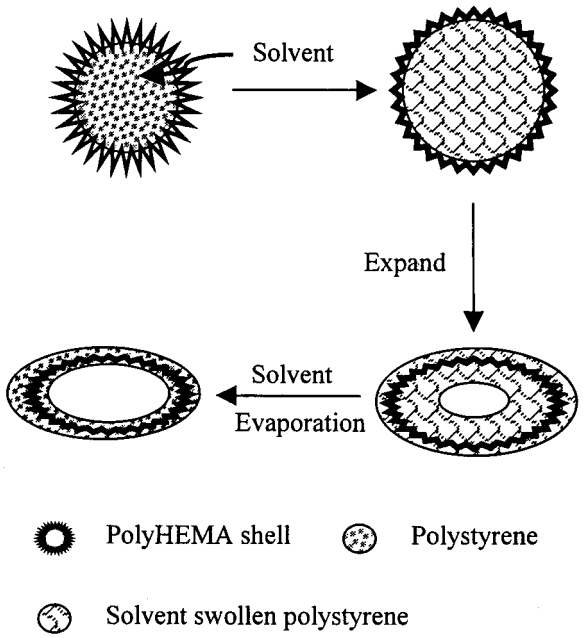

Figure 3. Schematic conversion of a latex sphere, the building block of a colloidal crystal, into a polymer loop, the building block of a polymer net.

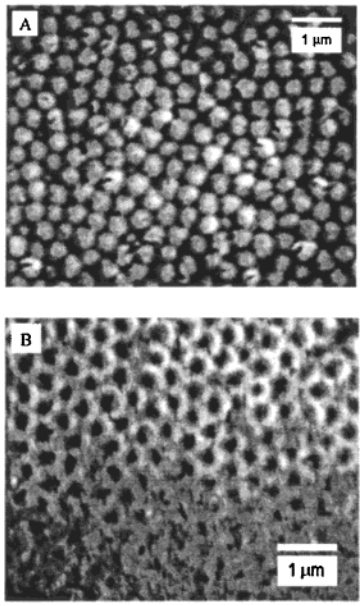

Figure 4. (A) Disordered film of 10% HEMA latex showing cracks on some spheres after exposure to styrene vapor for less than 10 min. (B) Colloidal crystal sample that was partially immersed in liquid styrene. The bottom (immersed) part of the sample appears featureless, whereas the top part shows a net.

solvent vapor localizes the transformation within the vicinity of each sphere. The center-to-center distance between the holes in the net shown in Figure 2C is the same as that between the particles in the colloidal crystal (Figure 2A). When the crystal is immersed into the solvent, the original structure is destroyed, as shown in Figure 4B. For similar reasons, a good solvent for both phases, such as chloroform, cannot effect the colloidal crystal-to-net conversion. We suggest that the morphological changes are driven by minimization of the free energy of the polymer−air interface, which is lower for swollen polystyrene than for polyHEMA. When

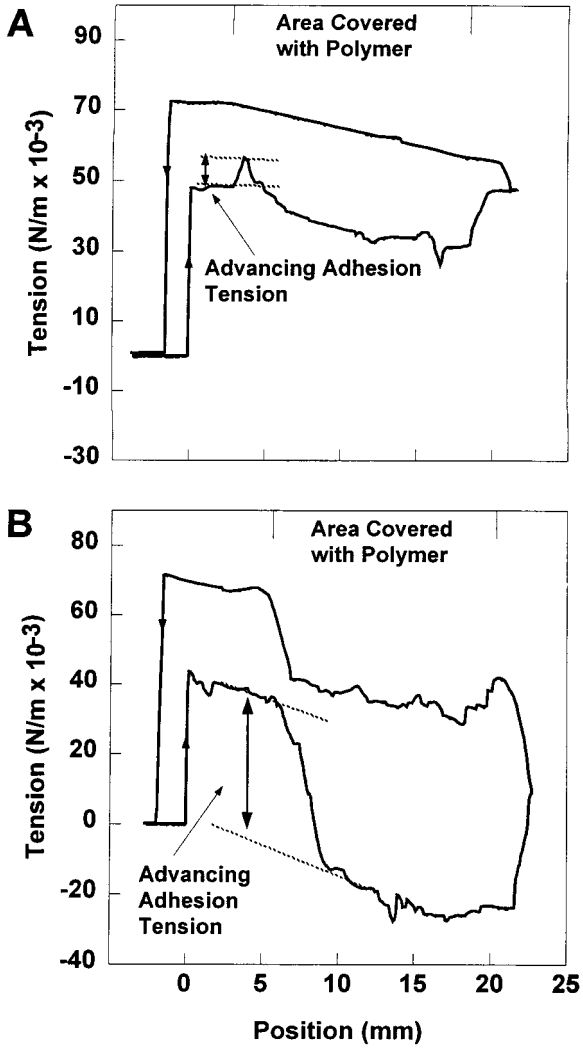

Figure 5. Wetting cycles for (A) a coloidal crystal and (B) a porous net of 10% HEMA copolymer coated on 22-mm-wide slides. Arrows on the curve pointing up indicate the plate advancing into the water, and arrows pointing down indicate the plate being removed from the water. The point where the plate first touches the water has been set arbitrarily as the zero position. Contact angles were calculated using the adhesion tension values indicated in the plots.[32]

the solvent evaporates from the net, the polymer morphology is a rigid polystyrene sheath around polyHEMA threads in the core. The whole polymer net is fused into one piece and is tougher than the colloidal crystal.

Wettability of the Films. The conversion of spheres with a polyHEMA-rich surface to a net with a polystyrene-rich surface is supported by wetting measurements of the films. Figure 5A and B shows changes in the adhesion tension of colloidal crystalline and net films measured by the dynamic Wilhelmy plate method[32] as slides coated with the film on both sides were lowered into and withdrawn from water. The adhesion tension is the product of the liquid surface tension and the contact angle. Contact angles were calculated using the adhesion tension values indicated in the plots by double-headed arrows. The increase of the adhesion tension when the water reached the colloidal crystalline polymer band, as shown in Figure 5A, indicates a water-wetting system with an advancing contact angle of less than 90° (calculated value = 85 ± 2°). The receding contact angle

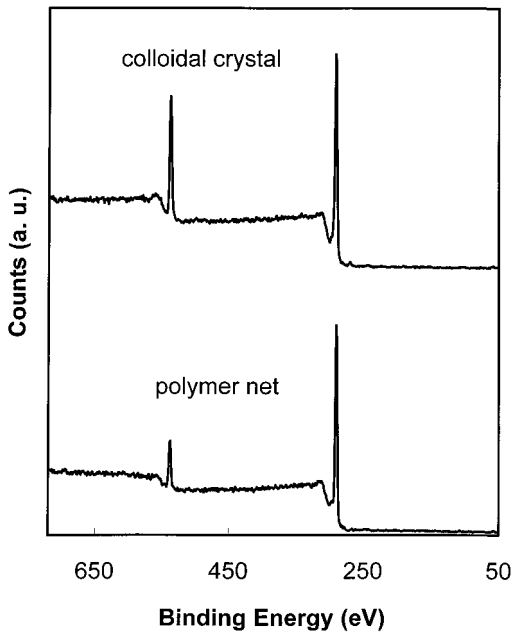

Figure 6. XPS spectra of a colloidal crystal and a porous net of a 10% HEMA copolymer.

is calculated to be 90 ± 2°. The big decrease of the adhesion tension when the water reached the polymer net band, shown in Figure 5B, indicates a nonwetting surface where the contact angle is greater than 90° (calculated value = 140 ± 3°). The receding contact angle is 109 ± 3°. Therefore, the polymer net surface is rich in polystyrene, and the colloidal crystal surface contains more polyHEMA. The large contact angle hysteresis of the net can be attributed to its rough surface with regular hexagonal features.[39−41]

X-ray Photoelectron Spectroscopy. Figure 6 shows XPS spectra for both a colloidal crystal and a polymer net. Peaks at 534 eV are due to oxygen atoms, and peaks at 286 eV are due to carbon atoms. The spectra indicate a much higher oxygen content at the surface of the colloidal crystal than at the surface of the net. Because only polyHEMA contains oxygen atoms, the oxygen peaks show that the colloidal crystal surface is richer than the net in polyHEMA. Water cannot be a major contributor to the oxygen peaks because the spectra were unchanged after the samples were left overnight in the analytical chamber under high vacuum. Because the electrons still escape from a few nanometers into the material, the oxygen peak from the net sample could be due to photoelectrons from the polyHEMA underneath a thin polystyrene coating.

Effect of Sphere Morphology on Conversion to the Net. To test how the latex core−shell structure affects the colloidal crystal-to-net conversion, we altered the sphere structure by starved-growth and seed-growth emulsion polymerizations.[42] In the seed-growth method, more styrene was added with stirring to a preformed latex, the mixture was stirred overnight at room temperature, new initiator was added, and the dispersion was heated to polymerize the monomer. Thus, all of the new monomer was absorbed into the particles, except for a small equilibrium amount in the aqueous phase, before polymerization resumed. The conditions and particle size information are in Table 2.

Table 2. Latexes from Starved-Growth and Seed-Growth Polymerizations[a]

		product particles		
growth method	initiator	styrene[b] (%)	diameter (nm)	calcd diameter (nm)
starved	$K_2S_2O_8$	96.3	444 ± 25	−
seed	$K_2S_2O_8$	95	468 ± 19	479
seed	AIBN	95	479 ± 6	479

[a] All preparations used 90/10 mol/mol styrene/HEMA in the first stage. The seed-growth experiments started with particles 380 ± 10 nm in diameter. [b] Mole percent after incorporation of all new monomer.

Because the amounts of monomer and original polymer can be measured accurately, the theoretical particle size after each growth stage can be calculated from eq 1, assuming that no new particles formed.

$$D_2 = (V_2/V_1)^{1/3} D_1 \quad (1)$$

In eq 1, V_1 is the volume of the seed polymer, V_2 is the volume of the polymer after polymerization of new monomer, D_1 is the diameter of the seed sphere, and D_2 is the diameter after the second stage polymerization. The experimental results in Table 2 agree well with the calculations, indicating a well-controlled seed-growth process.

There were two stages of the starved-growth process. In the first stage, a mixture of 90 mol % styrene and 10% HEMA was polymerized for 3 h as usual. In the second stage, an amount of styrene equal to twice the amount used in the first stage was added to the polymerizing dispersion using a syringe pump over a 2-h period. At the start of the second stage, most of the first batch of monomer had been consumed, and some initiator remained. The starved-growth method did not allow time for the new styrene monomer to reach an equilibrium state swollen into the particles. The new monomer polymerized near the particle surface as soon as it was absorbed.

Figure 7A is a TEM image of the product of the starved-growth polymerization. The particles are roughly spherical, but their surfaces are very bumpy. Figure 7B and C shows the products of seed-growth polymerizations initiated by persulfate and AIBN, respectively. The particle surfaces are smooth. All three samples formed colloidal crystals by evaporative deposition, but the particles from starved growth appear deformed, as shown in Figure 7D. When treated with styrene vapor, only the colloidal crystal of particles from the seed-growth polymerization initiated by AIBN within the particles was converted to a polymer net.

Recalling our model, the critical structure for the colloidal crystal-to-net transformation is a continuous polyHEMA-rich shell on a polystyrene-rich core. PolyHEMA is a rigid skeleton that prevents total collapse of the material during styrene vapor treatment. During starved-growth polymerization, new polystyrene chains are initiated in the aqueous phase, and oligomers with

(39) Fadeev, A. Y.; McCarthy, T. J. *Langmuir* **1999**, *15*, 3759−3766.
(40) Oener, D.; McCarthy, T. J. *Langmuir* **2000**, *16*, 7777−7782.
(41) Chen, W.; Fadeev, A. Y.; Hsieh, M. C.; Oener, D.; Youngblood, J.; McCarthy, T. J. *Langmuir* **1999**, *15*, 3395−3399.
(42) Lovell, P. A., El-Aasser, M. S., Eds. *Emulsion Polymerization and Emulsion Polymers*; John Wiley and Sons: Chichester, England, 1997.

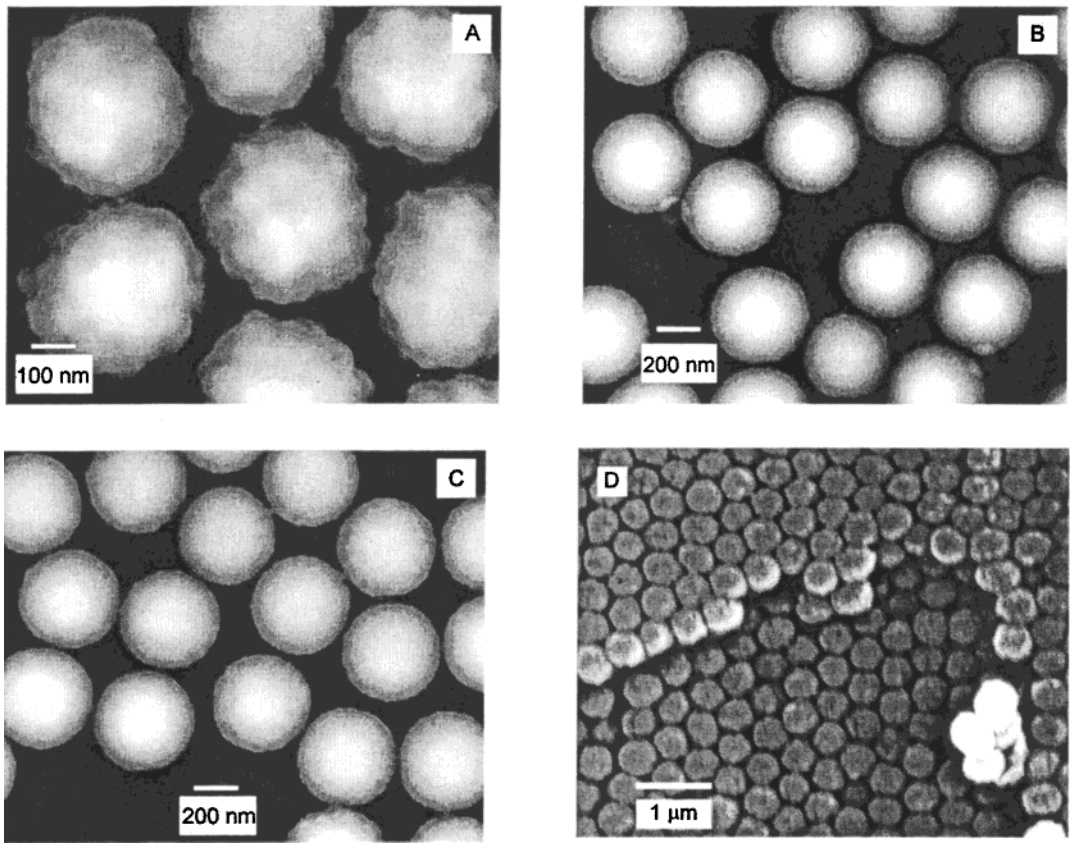

Figure 7. Electron microscopic images of the latexes of Table 2. (A) TEM image of the starved-growth sample. (B, C) TEM images of the seed-growth samples initiated with persulfate and AIBN, respectively. (D) SEM image of a colloidal crystal of the starved-growth latex.

sulfate end groups are captured by particles. Because of the size and charged ends of the oligomers, propagation continues near the particle surface to produce new homopolystyrene that does not diffuse to the particle core and leaves bumps on the particle surface. In the seed-growth polymerizations, styrene monomer is absorbed into the core of the particle before new polymerization is initiated. Initiation of the second-stage polymerization with persulfate gave larger spherical particles that formed colloidal crystalline films, but the films did not transform into a net. Initiation with AIBN gave particles that formed colloidal crystals and did convert to nets. The difference lies in the method of initiation. When initiated in the aqueous phase, the new styrene oligomers that are captured by the particles still cannot diffuse to the core, and the new polystyrene forms near the surface. When initiated in the swollen core, the new polystyrene forms in the core, leaving the polyHEMA-rich phase on the surface. This interpretation of the morphologies of the particles from starved-growth and seed-growth polymerizations is consistent with previous kinetic and electron microscopic investigations of core−shell latexes.[42−44]

Comparison with Related Materials. Surface rearrangements of films of HEMA−styrene block copolymers, which have domain sizes on the order of 10 nm, also have been detected by XPS and by contact angle measurements after alternating exposures to water and air.[45,46] Soaking in water brings the polyHEMA block to the surface, and annealing in air brings the polystyrene block to the surface. However, the scale of these phase conversions is 10 times smaller than ours, and the polymer films are nonporous.

There are many ways to make porous materials. A poly(styrene-*b*-L-lactide) having the morphology of polylactide cylinders in a polystyrene matrix has been transformed into a porous polystyrene by degrading the polylactide.[47] The pores are vertical channels of about 10-nm diameter. The synthesis of inverse opals requires multiple steps of self-assembly of the template colloidal crystal, filling of the interstitial voids with a new liquid, hardening of the material in the interstices, and removal of the template by chemical erosion or calcination. The holes obtained in this way are more uniform, and the syntheses are more difficult than ours.[23,24] Polymer membranes for use as filters are commonly made by thermal gelation, solvent evaporation, imbibition of water vapor, and polymer precipitation by immersion in a nonsolvent bath.[2] Such membranes are usually not three-dimensionally uniform, and the pore sizes have a relatively broad distribution.

Compared with other methods of creating porous materials, solvent treatment of a colloidal crystalline film method is simple. Moreover, the final structure is

(43) Sundberg, E. J.; Sundberg, D. C. *J. Appl. Polym. Sci.* **1993**, *47*, 1277.
(44) Winzor, C. L.; Sundberg, D. C. *Polymer* **1992**, *33*, 3797.
(45) Lewis, K. B.; Ratner, B. D. *J. Colloid Interface Sci.* **1993**, *159*, 77.
(46) Senshu, K.; Yamashita, S.; Ito, M.; Hirao, A.; Nakahama, S. *Langmuir* **1995**, *11*, 2293.
(47) Zalusky, A. S.; Olayo-Valles, R.; Taylor, C. J.; Hillmyer, M. A. *J. Am. Chem. Soc.* **2001**, *123*, 1519.

three-dimensionally ordered. However, preparation of the colloidal crystal is slow and requires a monodisperse colloid. The new method should be applicable to a wide range of copolymer latexes that are composed of a hydrophobic monomer and a hydrophilic monomer. We plan to explore its generality.

Acknowledgment. We thank the National Science Foundation (DMR-9812523) for financial support and Terry Colberg and Phoebe Doss for assistance with the electron microscopy.

CM010255R